Int J Adv Manuf Technol (2009) 42:1175–1186
DOI 10.1007/s00170-008-1668-1

ORIGINAL ARTICLE

# Study on the convection heat transfer coefficient of coolant and the maximum temperature in the grinding process

**B. Lin · M. N. Morgan · X. W. Chen · Y. K. Wang**

Received: 11 October 2007 / Accepted: 10 July 2008 / Published online: 11 November 2008


**Abstract** Grinding fluid is typically applied in order to achieve reduced surface grinding temperatures, improved workpiece surface integrity, and extended wheel life compared to that which can be achieved in the dry situation. This paper presents the results of an investigation concerned with methods to determine the value of the convection heat transfer coefficient. The work is based on the theory of fluid dynamics and heat transfer that are used to describe the heat transfers within the grinding zone under different grinding conditions. The simulation research is made by means of the FEM for the wet grinding temperature distribution, and the three-dimensional topology map of the temperature distribution is obtained. Temperature is measured with the clamped thermocouple in different grinding conditions. The experimental result is approximately suitable to the simulated result. The simplicity and accuracy of the method allow the application to a wide range of grinding regimes from shallow-cut to high-efficiency deep grinding.

**Keywords** Grinding · Coolant · Convection heat transfer coefficient · Temperature

B. Lin (✉) · X. W. Chen · Y. K. Wang
Key Laboratory for Advanced Ceramics and Machining Technology of Ministry of Education, Tianjin University, Tianjin, China
e-mail: linbinph@tju.edu.cn

M. N. Morgan
Advanced Manufacturing Technology Research Laboratory (AMTReL), General Engineering Research Institute, Liverpool John Moores University, Liverpool, UK

**Nomenclature**

| | |
|---|---|
| $a_e$ | real depth of cut |
| $b$ | width of cut |
| $c$ | specific heat capacity |
| $C$ | temperature constant for workpiece conduction |
| $d$ | diameter |
| $d_e$ | effective wheel diameter |
| $d_s$ | wheel diameter |
| $d_w$ | workpiece diameter |
| $e_c$ | specific energy |
| $e_{ch}$ | specific chip energy |
| $E_s$ | modulus of elasticity of the grinding wheel |
| $E_w$ | modulus of elasticity of the workpiece |
| $F_n$ | normal grinding force |
| $F_t$ | tangential grinding force |
| $h_{eq}$ | equivalent chip thickness |
| $h_f$ | fluid convection factor |
| $h_w$ | workpiece convection factor |
| $k$ | thermal conductivity |
| $k_g$ | thermal conductivity of abrasive grain |
| $l$ | half-width of heat source |
| $l_c$ | theoretical contact length |
| $l_g$ | geometric contact length |
| $l_f$ | contact length between acted on by a normal force |
| $P$ | grinding power |
| $P'$ | specific grinding power |
| $P_e$ | Peclet number |
| $h_w$ | heat flux to the chips |
| $q_f$ | heat flux to the fluid |
| $q_s$ | heat flux to the wheel |
| $q_w$ | heat flux to the workpiece |
| $Q_w$ | volumetric material removal |
| $Q'_w$ | specific volumetric material removal |
| $r_0$ | effective radius of contact of the abrasive grains |
| $R_r$ | roughness factor |

| | |
|---|---|
| $R$ | fraction of heat entering a process element |
| $R_w$ | fraction of total grinding heat entering the workpiece |
| $R_{ws}$ | fraction which enters the workpiece of that heat shared by workpiece and wheel |
| $T_{max\ dry}$ | maximum calculated temperature, dry grinding |
| $T_{max\ wet}$ | maximum calculated temperature, wet grinding |
| $T_{mp}$ | melting point temperature |
| $v_w$ | work speed |
| $v_s$ | wheel speed |
| $\alpha$ | thermal diffusivity |
| $\beta$ | thermal property |
| $\rho$ | mass density |
| $\mu$ | grinding friction coefficient |
| $\upsilon_s$ | Poisson's ratio of the grinding wheel |
| $\upsilon_w$ | Poisson's ratio of the workpiece |

## 1 Introduction

Convective cooling has a major influence on the removal of grinding heat from the grinding zone, it is necessary to reduce the risk of thermal damage to the workpiece surface. This is generally desirable in all grinding regimes, including shallow-cut grinding, creep-feed grinding, and high-efficiency deep grinding (HEDG) [1, 2]. The cooling efficiency can be quantified by the convection heat transfer coefficient, $h_f$, of the coolant in the grinding zone. The value of $h_f$ is a critical variable of the process and determines the amount of heat convected from the contact zone and the subsequent workpiece surface temperature. Predictive temperature models, used for the control of workpiece surface integrity, require a value of $h_f$ as an input parameter and it is, therefore, preferable that an accurate value of the convective coefficient of the coolant in the grinding zone be known. Unfortunately, it is not easy to measure or calculate this value, and even the order of magnitude estimation is considered to be difficult. Therefore, most previous research has concentrated on the energy partition of the total grinding heat in order to estimate the workpiece surface temperature, while the energy partition coefficient is usually obtained by matching theoretically and experimentally determined temperatures within the grinding zone [3–5]. Some complex thermal models have also been developed by coupling the heat transfer between grains, workpiece, and coolant in which the coolant is assumed to be solid and moving at the wheel speed [6, 7].

In this paper, the value of the convection heat transfer coefficient of the fluid through the grinding zone will be determined by fluid dynamics and the theory of heat conduction. The analysis also assesses the effects of grinding variables on the value of the convection coefficient. The maximum contact temperature is predicted, using the method of Rowe and colleagues [8–11]. The results are in good agreement with that obtained from experimental measurements and 3-D finite element (FE) simulation results.

## 2 Previous work

There have been many papers published on the partitioning of the total grinding heat but here it is intended only to mention the key papers which are critical to the understanding of the new approach. The most important paper which laid the foundation for almost all later work was the paper on moving heat sources by Jaeger [12]. The moving band source model has been shown to be a good basis for modeling the shallow-cut grinding process [9, 10]. The solution of Fourier's Law of heat conduction applied to the sliding plane heat source situation provides the basis for almost all analyses of conduction of heat into the workpiece. The solution relates the heat flux (rate of heat per unit area) entering the workpiece and the temperatures within and on the workpiece. The multitude of short intense energy inputs which arise from all the grain–workpiece interactions taken together are usually assumed to be equivalent to a uniform band heat source moving along the workpiece at speed.

Using the definition of the Dirac delta function, Wen Liang Kuo and Jen Fin Lin obtained the temperature rise solution for a point heat source. It can be applied to predict the three-dimensional temperature rise distributions in the workpiece [28].

In an early paper by Outwater and Shaw [13], the heat transfer to the workpiece was modeled as a sliding heat source at the shear plane so that part of the heat is conducted into the workpiece and part into the chip. Of course, sliding also takes place between the chip and the abrasive grain so that part of the heat is conducted into the grain. Maris and Snoeys suggested that 70–80% of the energy is applied to the workpiece and 15–20% is applied to the chip and the grinding wheel although the heat to the chip and to the wheel could not be accurately established [14]. Pavel and Srivastava discussed the heat partition coefficients in grinding of 52100 steel using $Al_2O_3$ and CBN wheels under wet as well as dry grinding conditions [29]. Malkin showed the effect of the grain wear flats and calculated the maximum heat convected from the workpiece zone by considering the chip removal rate and the energy required to raise the material removed to melting temperature [4]. Malkin pointed out that there is a limit to the shear zone energy which can be carried away by the chips. This limit is the material melting energy and ferrous materials are approximate 6 J $mm^{-3}$. The total grinding energy is converted into heat. In most grinding processes, it

is safe to assume that the total grinding energy is much greater than the melting energy. Des Ruisscaux and Zerkel extended the Jaeger model to account for the superposition of a surface cooling effect of the coolant [15]. The paper also acknowledged the difficulty of determining and applying a convection coefficient which is different in the grinding zone from the surrounding area but pointed out the importance of cooling in this region.

Traditionally, there are two methods to estimate or measure the convection coefficient. The first method is an empirical method. It is usual for fluid convection to be related to the mean temperature, rather than the maximum temperature in the contact plane. When coolant is water-based fluids, the convection factor may be adjusted simply to a value, for example, of $h_f$=6,700 W/m$^2$K where the reduced convection factor allows for the fact that the maximum temperature is used in the calculation rather than the mean temperature. When the coolant is neat oils, the reduced convection coefficient assumed is 2,700 W/m$^2$K. The heat flux to the fluid can, therefore, be expressed approximately as:

$$q_f = h_f \times T_{max} | T_{max} \leq Tb \text{ or } q_f = 0 | T_{max} \geq Tb. \quad (1)$$

The value of $q_f$ from Eq. 1 depends on whether boiling conditions apply or not. Under nonboiling conditions, the first term is used, whereas under boiling conditions, the zero term is used. This means it is necessary to calculate the maximum temperature for both cases to determine which solution is appropriate. Unfortunately, convection factors for the grinding situation are not readily available. There is obvious uncertainty in the estimates of the fluid convection factors.

A further method used to estimate the cooling effect of the fluid is based on the 'fluid wheel' assumption. This approach has been claimed to give reasonable agreement with experiment in particular cases under nonboiling conditions [5]. The assumption in this case is that a layer of fluid traveling at wheel speed effectively covers practically the contact zone. Using the triangular sliding heat source and the fluid wheel assumption:

$$h_f = 0.94 \times \beta_f \times \sqrt{\frac{v_s}{l_c}}. \quad (2)$$

Equation 2 shows that the convection coefficient for fluid cooling reduces as contact length increases whereas the former assumption based on experiments for flow along a surface is for a constant convection coefficient.

Verkerk investigated the real contact length $l_c$ in grinding by measuring the heat pulses due to the transition of grains past a thermocouple embedded in the workpiece [16]. It was found that the real contact length was substantially greater than the geometrical value. The grinding contact area required for the determination of the heat flux is the product of the grinding width and the contact length. This means that the band heat source will be much wider and the heat flux to the workpiece will be much lower for deformable wheels than for a rigid grinding wheel and the maximum grinding zone temperature is correspondingly reduced.

In 1993, Rowe and Qi found that the contact length could be predicted based on the combination of the geometric contact length based on depth of cut and the elastic contact length based on the forces and deflections [17].

Werner et al. used finite element analysis to model heat flows to the workpiece, wheel, chips, and fluid in creep grinding. This was one of the first attempts to model the effect of all four heat sinks simultaneously [18].

Rowe and Morgan adopted aspects of the previous works in that the coolant effects and the maximum chip convection effects were used to modify the energy applied at the grain–workpiece interaction and the result compared with results obtained without these effects [9]. The effect of a deformable wheel was also included. A key feature of this work was the determination of the partitioning factor based on a simultaneous solution of the conduction into the grinding wheel and into the workpiece assuming an equal average temperature in the grinding contact zone. In later papers, it was shown that it was important to combine the effect of the four heat sinks but also that a simpler and more accurate result is achieved if the wheel–workpiece contact is modeled as a set of discrete contacts [10, 11].

It can be seen that most research presented above has concentrated on the energy partition of the total grinding heat. The energy partition coefficient and convection/conduction factors have been obtained by matching theoretical and experimentally determined temperatures within the grinding zone. It cannot be completely satisfactory in representing the convection heat transfer coefficient of coolant within the grinding zone.

Rowe and Morgan's analysis provides the basis for the prediction of workpiece temperatures in grinding which previously could not be achieved satisfactorily. In this paper, the Rowe and Morgan's thermal model and the model of the convection heat transfer coefficient estimated below will be used to predict the workpiece temperatures in grinding.

## 3 Derivation of a model for calculation of the convection heat transfer coefficient

The following section describes how the analytical model for the calculation of the convection heat transfer coefficient is derived from the coupling of fluid dynamics and the theory of heat conduction. Figure 1 shows the typical surface grinding contact condition and temperature conduc-

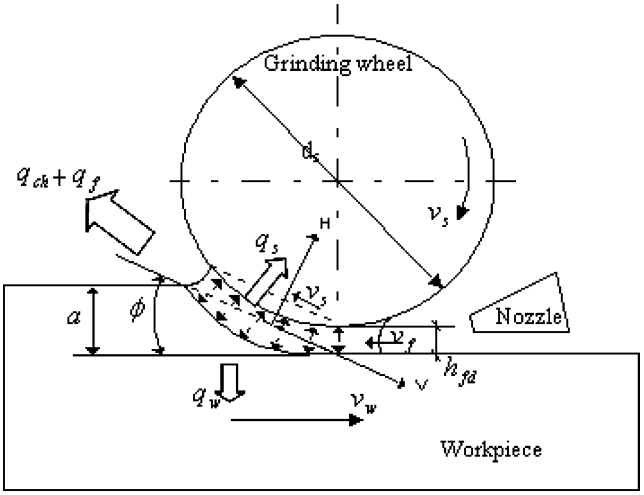


**Fig. 1** Illustration of fluid application in surface grinding

tion between the wheel and the workpiece. The heat generated is distributed to the workpiece, wheel, fluid, and chips. In order to facilitate the fluid flow analysis, the following assumptions are made [19]:

- Fluid motion is characterized by average velocity.
- The wheel is adequately dressed to have uniform surface form.
- Convection is the major mode of heat transfer.
- Useful flow takes place in the contact area without side flow.
- The fluid flow is predominantly laminar.

We now proceed to build up a semiempirical equation based on the theory of conduction of heat in solids [20]:

$$Nu = 0.664 \times \mathrm{Re}^{1/2}\,\mathrm{Pr}^{1/3} \tag{3}$$

where *Re* is the Reynolds number, *Pr* is the Prandtl number, and *Nu* is the Nusselt number:

$$\mathrm{Re} = \frac{\rho f v_{\mathrm{av}} l_{\mathrm{c}}}{\mu_{\mathrm{f}}}; \quad \mathrm{Pr} = \frac{\mu_{\mathrm{f}} C_{\mathrm{f}}}{k_{\mathrm{f}}}; \quad Nu = \frac{h_{\mathrm{f}} l_{\mathrm{c}}}{k_{\mathrm{f}}} \tag{4}$$

where $\rho_{\mathrm{f}}$ is the fluid density, $\nu_{\mathrm{av}}$ is the average fluid velocity in grinding gap, $l_{\mathrm{c}}$ is the contact length, $\mu_{\mathrm{f}}$ is the dynamic viscosity, $k_{\mathrm{f}}$ is the thermal conductivity of the fluid, and $C_{\mathrm{f}}$ is the specific heat of the fluid. The thermal and kinematic properties of the fluid were obtained from reference [21].

Substituting for the fluid properties and combining Eqs. 3 and 4, the convection heat transfer coefficient $h_{\mathrm{f}}$ can be expressed as:

$$h_{\mathrm{f}} = G\sqrt{\frac{v_{\mathrm{av}}}{l_{\mathrm{c}}}} \tag{5}$$

where $\nu_{\mathrm{av}}$ is the average velocity of the fluid through the grinding zone. $G$ is a constant; $l_{\mathrm{c}}$ is the contact length for both the wheel and the workpiece:

$$G = 0.664\rho^{\frac{1}{2}} C_{\mathrm{p}}^{\frac{1}{3}} \mu^{-\frac{1}{6}};\; l_{\mathrm{c}} = \left[R_{\mathrm{r}}^2 8F'_{\mathrm{n}}(k_{\mathrm{s}} + k_{\mathrm{w}})d_{\mathrm{s}} + ad_{\mathrm{s}}\right]^{0.5}. \tag{6}$$

In accordance with the assumptions and neglecting the effects of wheel porosity, the wheel–workpiece contact area through the fluid can, therefore, be considered as two parallel plates with a constant separation (see Fig. 1). The average velocity from the Navier–Stokes equation for steady-state motion applied to this case yields [22]:

$$\frac{\partial^2 v}{\partial H^2} = \frac{1}{\mu_{\mathrm{f}}}\frac{\partial p}{\partial u} \tag{7}$$

where $u$ is the fluid flow velocity in direction $v$ and $\mu_{\mathrm{f}}$ is the dynamic viscosity of the grinding fluid. The boundary conditions are defined as:

$$u = (v_{\mathrm{f}} + v_{\mathrm{w}})\cos\phi \,\text{at}\, H = 0;\; u = v_{\mathrm{s}} - v_{\mathrm{f}}\cos\phi \,\text{at}\, H = h_{\mathrm{fd}}$$

where $h_{\mathrm{fd}}$ is the fluid film thickness within the grinding zone.

The pressure gradient can be considered as zero based on the previous assumptions. Solving Eq. 5 for the given boundary conditions, the velocity of the fluid distributed in a section can be expressed as:

$$\begin{aligned} u &= \frac{1}{2\mu}\frac{\partial p}{\partial u}\left(H^2 - Hh_{\mathrm{fd}}\right) + \left[v_{\mathrm{s}} - (2v_{\mathrm{f}} + v_{\mathrm{w}})\cos\phi\right]\frac{H}{h_{\mathrm{fd}}} \\ &\quad + (v_{\mathrm{f}} + v_{\mathrm{w}})\cos\phi \\ &= \left[v_{\mathrm{s}} - (2v_{\mathrm{f}} + v_{\mathrm{w}})\cos\phi\right]\frac{H}{h_{\mathrm{fd}}} + (v_{\mathrm{f}} + v_{\mathrm{w}})\cos\phi. \end{aligned} \tag{8}$$

The average fluid velocity in the section, calculated from Eq. 8 is:

$$v_{\mathrm{av}} = \frac{2}{A}\int_A udA \tag{9}$$

where $A$ is the average transect area of the wheel–workpiece gap.

By substituting Eqs. 6 and 9 into Eq. 5, the coefficient $h_{\mathrm{f}}\left(v_{\mathrm{s}}, v_{\mathrm{f}}, v_{\mathrm{w}}, a_{\mathrm{p}}, f_{\mathrm{fd}}, l_{\mathrm{c}}\right)$ can be solved for particular experimental conditions. The film thickness of the fluid $h_{\mathrm{fd}}$ between the wheel and the workpiece can be estimated by analyzing the depth of fluid penetration on the wheel surface and the surface topography between the wheel and the workpiece [23].

## 4 Thermal analysis

The knowledge of the value of the convection heat transfer coefficient allows for the maximum contact temperature to

be estimated. In grinding, the heat generated at the workpiece–wheel interface is distributed between the workpiece, wheel, chips, and fluid. The grinding temperatures are dependent on the heat flux generated in the contact zone. In order to calculate the grinding temperatures, it is necessary to understand the heat flux distribution in the grinding zone.

### 4.1 General relations

The basis of the model is given below. The relationship between power, force, and wheel speed is:

$$P = F_t \times v_s. \tag{10}$$

Volumetric material removal is given by:

$$Q_w = a_e \times v_w \times b. \tag{11}$$

The relationships above expressed in specific terms are specific power:

$$P' = \frac{F_t \times v_s}{b} \tag{12}$$

and specific volumetric material removal:

$$Q'_w = a_e \times v_w. \tag{13}$$

Further important quantities are the total specific grinding energy:

$$e_c = \frac{F_t \times v_s}{Q_w} \tag{14}$$

and equivalent chip thickness:

$$h_{eq} = a_e \times \frac{v_w}{v_s}. \tag{15}$$

### 4.2 Energy partitioning

In grinding, the heat generated at the workpiece–wheel interface is distributed between the workpiece, wheel, chips, and fluid. The grinding temperatures are dependent on the heat flux generated in the contact zone. In order to calculate the grinding temperatures, it is necessary to specify the heat flux distribution in the grinding zone. The total heat flux $q_t$ is the sum of the four flux components.

$$q_t = q_w + q_s + q_{ch} + q_f \tag{16}$$

where:

$$q_t = \frac{P}{b \times l_c} = e_c \times \frac{Q'_w}{l_c}. \tag{17}$$

The heat flux to the workpiece, wheel, fluid, and chips may be expressed in terms of convention/conduction factors defined in relation to the maximum material melting temperature as follows:

$$q_w = h_w \times T_{max}, \tag{18}$$

$$q_s = h_s \times T_{max}, \tag{19}$$

$$q_f = h_f \times T_{max}, \tag{20}$$

$$q_{ch} = h_{hch} \times T_{mp}. \tag{21}$$

The maximum workpiece temperature in the contact plane based on the theory of the sliding heat source for one-dimensional conduction is defined as:

$$T_{max} = C \times \frac{q_w}{\beta_w} \times \sqrt{\frac{l_c}{v_w}}. \tag{22}$$

The convection factor for the workpiece may be expressed as:

$$h_w = \frac{\beta_w}{C} \times \sqrt{\frac{v_w}{l_c}} \tag{23}$$

where the thermal property and theoretical contact length $l_c$ are given by:

$$\beta_w = \sqrt{k_w \times \rho_w \times c_w}, \tag{24}$$

$$l_c = l_g = \sqrt{a_e \times d_e}. \tag{25}$$

The effective wheel diameter is obtained from:

$$\frac{1}{d_e} = \frac{1}{d_s} \pm \frac{1}{d_w}. \tag{26}$$

In surface grinding, the heat source model gives a value for $C$ approximately equal to unity, but precise values depend on the value of $Pe$ (Peclet number):

$$P_e = \frac{v_w \times l_c}{4 \times \alpha_w}. \tag{27}$$

Since:

$$l = \frac{l_c}{2} \tag{28}$$

and

$$\alpha_w = \frac{k_w}{\rho_w \times c_w}. \tag{29}$$

The convection factor for the abrasive grains, $h_s$, can be evaluated $h_w$ from the partition ratio between wheel and workpiece:

$$h_s = h_w \times \left[\frac{1}{R_{ws}} - 1\right]. \tag{30}$$

The workpiece–wheel partition ratio $R_{ws}$ is expressed as:

$$R_{ws} = \frac{q_w}{q_w + q_s} = \frac{h_w}{h_w + h_s} = \left[1 + \frac{0.974 \times k_g}{\beta_w \times \sqrt{r_0 \times v_s}}\right]^{-1} \quad (31)$$

where $r_0$ represents an effective radius of contact of the abrasive grains. The value of $r_0$, which is equal to 15 μm, is a sensible value for a reasonably sharp wheel. For a given abrasive type, the ratio does not change significantly [24].

The flux to the chip $e_{ch}$ is assumed to be close to the limiting chip energy, which is the value required to raise the temperature of the chip material to melting [25]. For ferrous materials, this value is approximately 6 J mm$^{-3}$. The flux to the chips can be expressed as:

$$q_{ch} = e_{ch} \times \frac{Q'_w}{l_c} \quad (32)$$

where the limiting chip energy is:

$$e_{ch} = \rho_w \times c_w \times T_{mp}. \quad (33)$$

The fluid convention factor $h_f$ is the most difficult parameter to estimate with any confidence, and from the above analysis, it can be shown that the fluid convection factor is given by:

$$h_f = G \times \sqrt{\frac{v_{av}}{l_c}}. \quad (34)$$

Two values of $T_{max}$ may be calculated from Eqs. 18, 19, and 21 using the convection factors from Eqs. 23, 30, and 34:

$$T_{max\,wet} = \frac{q_t - q_{ch}}{\frac{h_w}{R_{ws}} + h_f} \quad (35)$$

and

$$T_{max\,dry} = \frac{q_t - q_{ch}}{\frac{h_w}{R_{ws}}}. \quad (36)$$

### 4.3 The grinding contact length

In predicting the temperature of the workpiece, it is very important to know the effective length of the heat source over which the energy conducts into the workpiece.

It has been found that the real contact length in grinding is often much greater than the geometric contact length $l_g$. An advanced theoretical solution for real contact length proposed by Rowe and Qi was [5]:

$$l_c^2 = l_f^2 + l_g^2 \quad (37)$$

where $l_f$ is the contact length between surfaces which is acted on by a normal force and $l_g$ is the geometric contact length defined by Eq. 25. The length $l_f$ is evaluated from:

$$l_f = \sqrt{8 \times F'_n \times (K_s + K_w) \times d_s} \quad (38)$$

where $F'_n$ is the specific normal force:

$$K_s = \frac{1 - v_s^2}{\pi \times E_s} \quad (39)$$

and

$$K_w = \frac{1 - v_w^2}{\pi \times E_w}. \quad (40)$$

Variables $K_s$ and $K_w$ are determined from the physical properties of materials in the contact. $\upsilon_s$ and $\upsilon_w$ are Poisson's ratios, $E_s$ and $E_w$ are the Young's modulus. The real contact length can be expressed using a surface roughness approach or a contact area approach. The first yields more faithful results in comparison with the experimental results [26]. Based on the roughness approach, the magnitude of the grinding contact length is represented as:

$$l_c = \sqrt{l_{fr}^2 + 1_g^2} = \sqrt{(R_r \times l_f)^2 + 1_g^2} \quad (41)$$

where $l_{fr}$ is the contact length for rough surfaces with normal force and $R_r$ is the roughness factor. The magnitudes of the roughness factor are acquired as experimental values from the tests. $R_r$ is sensitive to the grinding conditions for some material combinations. For the general analysis of the grinding conditions where measured values of the roughness factor are not available, it is suggested that the value $R_r$ is equal 7.

Combining Eqs. 25, 38, and 41 yields the relationship:

$$l_c = \sqrt{8 \times R_r^2 \times F'_n \times (K_s + K_w) \times d_s + a \times d_e}. \quad (42)$$

Equation 42 determines the contact length between the wheel body and workpiece taking account not only the elastic deflection and geometric effect but also the roughness of both surfaces in the contact.

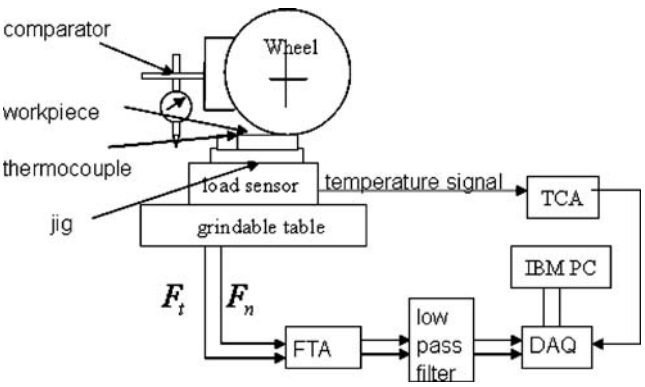


**Fig. 2** Grinding measurements and monitoring system. *FTA* force table amplifier, *DAQ* data acquisition and processing, *TCA* thermocouple amplifier

## 5 Experimental setting

The workpiece surface temperature in surface grinding was measured by using a 'grindable' thermocouple exposed at the workpiece surface. The thermocouple consisted of a chromel foil insulated at either side by mica and was housed in a premachined slot in the workpiece. In this configuration, the workpiece acts as the other thermocouple pole. The thickness of the measuring junction was approximately 25 μm. This configuration gave high-quality signals in both dry and wet grinding. Calibration of the thermocouple at temperatures below 100°C was obtained by pouring hot water over the measuring junction and recording the thermocouple output voltage. Calibration at higher temperatures was obtained in-process by comparing the sensor output with a specially configured standard thermocouple housed within the same plane of the workpiece. A signal from the thermocouple was obtained during a single pass of the grinding wheel over the workpiece. As the grinding wheel passed the measuring junction, the thermocouple poles connected because of plastic deformation of the workpiece material in the grinding zone. In order to minimize signal noise, the output of the thermocouple was connected to an amplifier located in close proximity to the workpiece.

The temperature measurement technique was implemented on a surface grinding machine. A schematic representation of the measuring system is shown in Fig. 2. The workpiece was housed in a jig containing an amplifier circuit. The jig was rigidly attached to a calibrated load sensor. The grinding wheel dimensions and rotational speed were measured for each grind. The workpiece speed was obtained by timing the normal force signal which was data logged to a PC. The contact length was computed from the product of the workpiece and the measured contact time. The surface temperature and grinding forces were recorded as the workpiece passed under the grinding wheel. The grinding power was computed from the product of the tangential force and the grinding wheel speed. The real depth of cut was measured before and after grinding by a mechanical gauge on the specially designed workpiece.

**Table 1** Grinding wheels (Altos) specification

| Parameters | Grinding wheel |
|---|---|
| Bore (mm) | 304.5 |
| Outer diameter(mm) | 500 |
| Width (mm) | 20 |
| Radial thickness (mm) | Solid |
| Maximum rated speed (rpm) | 6,000 |
| Grit | B252 |
| Porosity | High |
| Body | Disc |

**Table 2** Dimensions and properties of workpiece materials

| | Symbol | Units | CI | M50 |
|---|---|---|---|---|
| Length | $L$ | mm | 60 | 60 |
| Width | $b$ | mm | 5 | 5 |
| Mass density | $\rho$ | kg $m^{-3}$ | 7,300 | 7,870 |
| Specific heat capacity | $c$ | J $kg^{-1}$ $K^{-1}$ | 511 | 437 |
| Thermal conductivity | $k$ | W $m^{-1}$ $K^{-1}$ | 53.7 | 25.7 |
| Thermal diffusivity | $\alpha$ | $m^2$ $s^{-1}$ $10^{-6}$ | 14.4 | 7.47 |
| Thermal property | $\beta$ | J $m^{-2}$ $s^{-1/2}$ $K^{-1}$ | 14,150 | 9,402 |
| Poisson's ratio | $\upsilon$ | – | 0.26 | 0.26 |
| Young's modulus | $E$ | $GN/m^2$ | 160 | 180 |
| Melting temperature | $T_{melt}$ | °C | 1,500 | 1,400 |

### 5.1 Grinding wheels

A high porosity and permeable ceramic aluminum oxide (Altos) wheel produced by Saint-Gobain Abrasives was used for all experiments (Table 1). The porosity value is 54%, the mass density is 1,723 kg $m^{-3}$, the specific heat capacity is 765 J $kg^{-1}$ $K^{-1}$, the thermal conductivity is about 35 W $m^{-1}$ $K^{-1}$ [27], the Poisson's ratio is 0.22, and the modulus of elasticity is 49.6 GN $m^{-1}$.

### 5.2 Ground materials

Narrow metal plates were used during shallow grinding tests. The dimensions and properties of the workpiece are shown in Table 2.

### 5.3 Coolants

A water-based coolant was used during the shallow grinding tests. The physical properties of the coolant, used in the thermal analysis, are given in the Table 3. Fluid delivery was realized by means of one cooling nozzle aimed into the contact area.

**Table 3** Properties of water-based coolant used in experiments

| | Symbol | Units | Quantity |
|---|---|---|---|
| Mass density | $\rho$ | kg $m^{-3}$ | 1,000 |
| Specific heat capacity | $c$ | J $kg^{-1}$ $K^{-1}$ | 4,200 |
| Thermal conductivity | $K$ | W $m^{-1}$ $K^{-1}$ | 0.56 |
| Thermal diffusivity | $\alpha$ | $m^2$ $s^{-1}$ $10^{-6}$ | 1.33 |
| Thermal property | $\beta$ | J $m^{-2}$ $s^{-1/2}$ $K^{-1}$ | 1,534 |
| Viscosity | $\mu$ | $m^2$ $s^{-1}$ $10^{-3}$ | 0.98 |

**Table 4** Grinding conditions

| | Symbol | Unit | Value |
|---|---|---|---|
| Wheel speed | $v_s$ | m/s | 36 |
| Work speed | $v_w$ | mm/s | 270 |
| Depth of cut | $a_e$ | mm | 0.01–0.06 |

### 5.4 Cutting conditions

The programmed depths of cut $a$, shown in Table 4, were established on the grinding machine manually and were set in the range $a$=0.01 to 0.06 mm with incremental steps of 0.005 mm. The real depth of cut $a_e$ was measured after each grinding trail by a mechanical gauge.

## 6 Review of results from grinding tests

All the acquired data from the experiments were entered into the thermal model described previously and used for the thermal analysis. The analysis employed the real contact length based on the model of Rowe and Qi [17].

A key aim of the tests was to validate the thermal model on the basis of acquired data from measurements. One of the most important issues is a comparison of measured and calculated grinding temperatures. Good correlation between measured and calculated temperature values is required if the model is to be used in other grinding operations. The calculated and experimental results are presented below. Measured temperature obtained during the tests is compared with the temperature obtained from the thermal analysis.

The analysis predicts that when cooling conditions are good, the measured temperature should lie in the theoretical values calculated for wet and dry grinding. The better the cooling conditions are, the closer the measured temperature comparing with the maximum calculated temperature is. A coolant was used in the grinding tests, so it was expected that the measured temperatures would be very close to the maximum temperatures calculated for the case of wet grinding. In reality, however, the fluid delivery system was not as efficient as needed, fluid delivery to the contact region was unsatisfactory, and some measured temperatures are closer to the maximum theoretical temperature for the case of dry grinding.

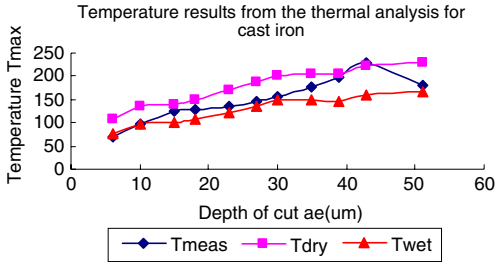


**Fig. 3** Comparison of estimated and measured temperatures in grinding, CI tests

The data from the cast iron tests is presented in Table 5. Measured temperatures are generally in the range of 100°C to 200°C. $P_w$ is the absolute value of the error between the $T_{wet}$ and the $T_{meas}$, so:

$$P_w = \frac{|T_{meas} - T_{wet}|}{T_{meas}}. \tag{43}$$

In the cast iron tests, the average value of $P_w$ is less than 14%, the maximum value of $P_w$ does not exceed 30%, and most values of $P_w$ are below 14%. The maximum of $P_w$ may be due to the measurement problems with the forces or

**Table 5** Calculated and experiments results, CI tests

| Results of CI tests | | | | | | | | | | | |
|---|---|---|---|---|---|---|---|---|---|---|---|
| Real $a_e$ (μm) | 6 | 10 | 15 | 18 | 23 | 27 | 30 | 35 | 39 | 43 | 51 |
| $F_t$ (N) | 8 | 11 | 13 | 15 | 18 | 21 | 23 | 25 | 26 | 29 | 32 |
| $F_n$ (N) | 20 | 23 | 27 | 32 | 37 | 43 | 48 | 52 | 54 | 60 | 66 |
| $P$ (W) | 288 | 396 | 468 | 540 | 648 | 756 | 828 | 900 | 936 | 1,044 | 1,152 |
| $e_c$ (J mm$^{-3}$) | 36 | 30 | 23 | 22 | 21 | 21 | 20 | 19 | 18 | 18 | 17 |
| $Q_w$ (mm$^{-3}$ s$^{-1}$) | 8 | 14 | 20 | 24 | 31 | 36 | 40 | 47 | 52 | 58 | 69 |
| $l_c$ (mm) | 3.04 | 3.49 | 3.99 | 4.36 | 4.8 | 5.19 | 5.47 | 5.8 | 6.03 | 6.34 | 6.79 |
| $h_f$ (W/m$^2$ K) | 56,405 | 52,646 | 49,230 | 47,113 | 44,886 | 43,176 | 42,029 | 40,809 | 40,052 | 39,051 | 37,743 |
| $T_{meas}$ (°C) | 69 | 96 | 126 | 127 | 136 | 147 | 157 | 178 | 199 | 230 | 180 |
| $T_{dry}$ (°C) | 108 | 134 | 138 | 151 | 169 | 189 | 200 | 206 | 204 | 223 | 229 |
| $T_{wet}$ (°C) | 78 | 97 | 100 | 109 | 122 | 137 | 149 | 149 | 147 | 161 | 166 |
| $P_w$ (%) | 13 | 1 | 21 | 14 | 10 | 7 | 5 | 16 | 26 | 30 | 8 |

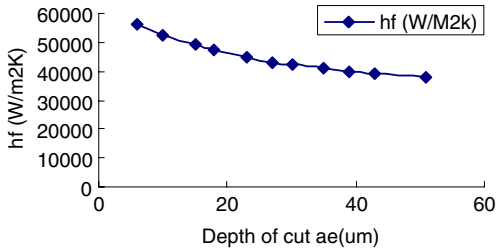


**Fig. 4** Effect of depth of cut on the convection heat transfer coefficient, CI tests

power. The measured temperatures do not exceed the theoretical temperatures for the case of dry grinding and often lay within the wet and dry values (Fig. 3).

The calculated results show that the values of the convection coefficient can be very high, much higher than the values previously reported. The values of the convection coefficient are seen to change with process parameters: real depth of cut (Fig. 4) and wheel speed, and decrease as the contact length increases.

Temperature simulation results generated by using finite element analysis in ANSYS 6.0 are also presented in Figs. 5, 6, and 7. In the FEA model, the surf152 element

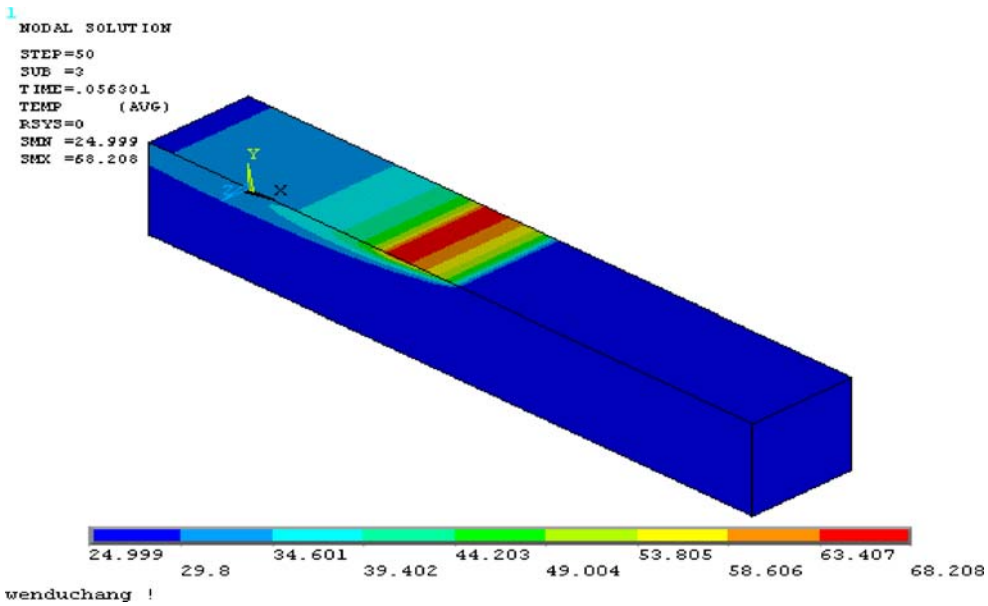


**Fig. 5** Temperature results at real depth cut of 6 μm by FEM, CI tests

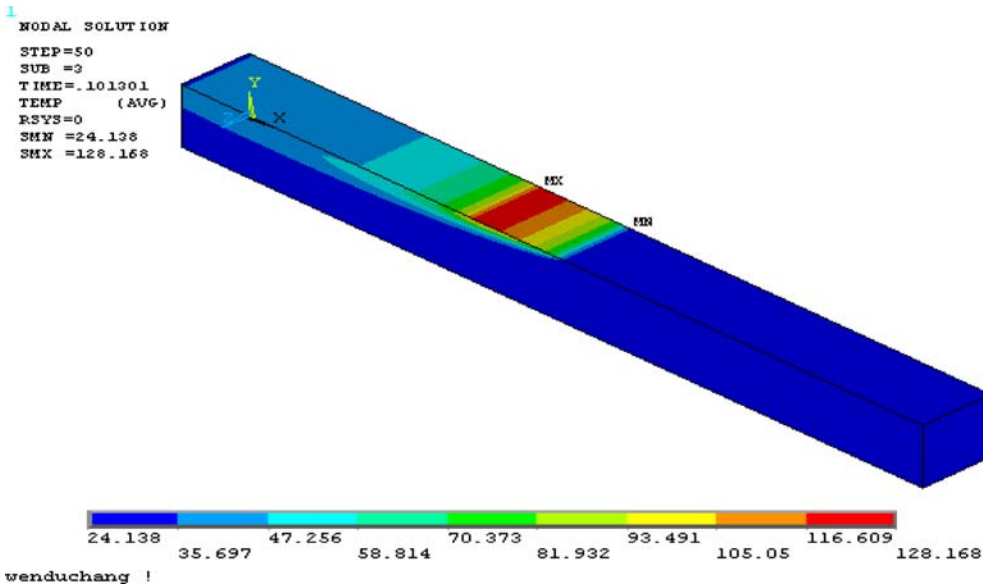


**Fig. 6** Temperature results at real depth cut of 30 μm by FEM, CI tests

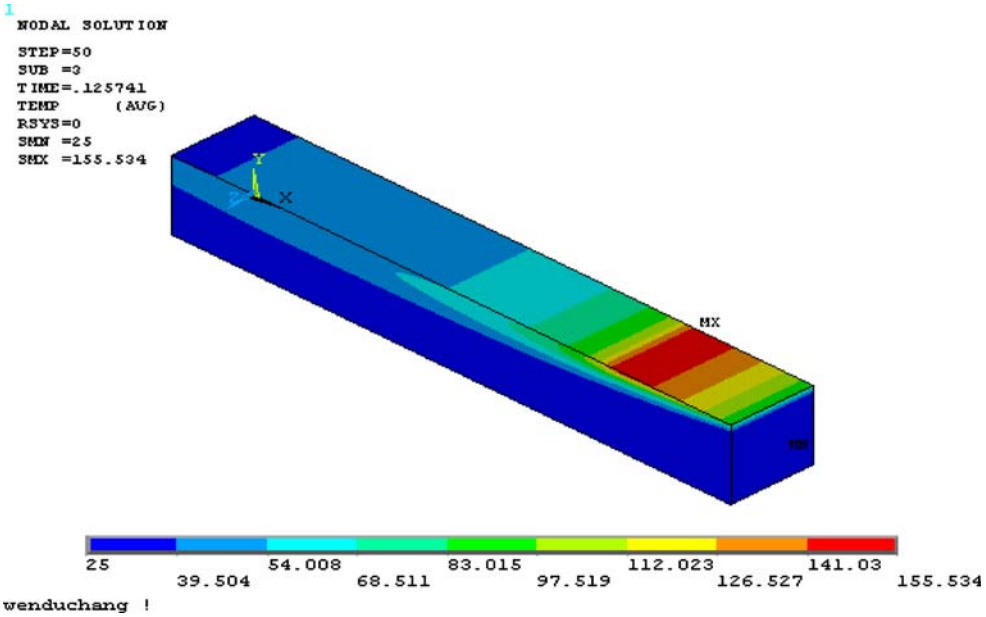


**Fig. 7** Temperature results at real depth cut of 51 μm by FEM, CI tests

**Table 6** Calculated and experiments results, M50 tests

| Results of M50 tests | | | | | | | | | | | |
|---|---|---|---|---|---|---|---|---|---|---|---|
| Real $a_e$ (μm) | 4 | 7 | 8 | 12 | 11 | 12 | 13 | 18 | 21 | 25 | 26 |
| $F_t$ (N) | 14 | 26 | 32 | 39 | 42 | 47 | 52 | 57 | 62 | 67 | 70 |
| $F_n$ (N) | 30 | 55 | 70 | 85 | 95 | 101 | 110 | 125 | 135 | 150 | 162 |
| $P$ (W) | 504 | 936 | 1,152 | 1,404 | 1,512 | 1,692 | 1,872 | 2,052 | 2,232 | 2,412 | 2,520 |
| $e_c$ (J mm$^{-3}$) | 93 | 99 | 107 | 87 | 102 | 104 | 107 | 85 | 79 | 71 | 72 |
| $Q_w$ (mm$^3$ s$^{-1}$) | 5.4 | 9.45 | 10.8 | 16.2 | 14.9 | 16.2 | 17.6 | 24 | 28 | 34 | 35 |
| $l_c$ (mm) | 3.35 | 4.5 | 5.03 | 5.64 | 5.86 | 6.06 | 6.32 | 6.86 | 7.18 | 7.62 | 7.89 |
| $h_f$ (W/m$^2$ K) | 53,856 | 46,378 | 43,859 | 41,401 | 40,614 | 39,956 | 39,121 | 37,561 | 36,705 | 35,621 | 35,013 |
| $T_{meas}$ (°C) | 400 | 510 | 473 | 573 | 600 | 610 | 683 | 687 | 604 | 628 | 700 |
| $T_{dry}$ (°C) | 285 | 457 | 534 | 607 | 647 | 713 | 773 | 804 | 851 | 886 | 910 |
| $T_{wet}$ (°C) | 186 | 298 | 348 | 396 | 422 | 465 | 504 | 524 | 554 | 577 | 593 |
| $P_w$ (%) | 20 | 6 | 27 | 34 | 3 | 17 | 9 | 5 | 2 | 13 | 27 |

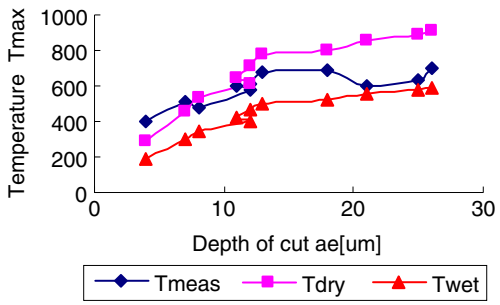


**Fig. 8** Comparison of estimated and measured temperatures in grinding, M50 tests

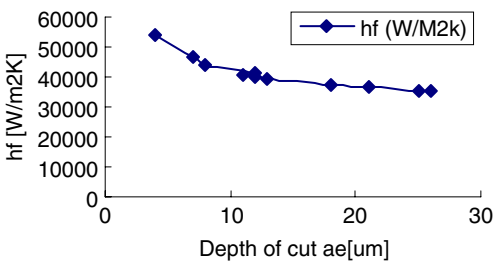


**Fig. 9** Effect of depth of cut on the convection heat transfer coefficient, M50 tests

was adopted and the heat flux and thermal and convection heat transfer coefficient were located in the element of grinding arc. The results show a good agreement with the theory. The value of the convection heat transfer coefficient used in the model is based on the coupled fluid dynamic and thermal model analysis.

The data from the tests with workpiece material M50 are presented in Table 6. The values of the convection coefficient obtained from the M50 tests are a little lower than those obtained from the CI tests. This is because the contact length in the M50 tests is lower than that in the CI tests. However, the results do not differ significantly because of the fixed wheel speed. Measured temperatures are generally in the range of 200°C to 600°C. In the M50 tests, the average value of $P_w$ is less than 13%, the maximum value of $P_w$ does not exceed 34%, and most values of $P_w$ are below 20%. As in the CI tests, the maximum of $P_w$ may be also due to the measurement problems with the forces or power. In most cases of this test, the measured temperatures do not exceed the theoretical temperatures for the case of dry grinding and often lie within the wet and dry values in Fig. 8. However, in the first two grinding tests, the measured temperatures exceed the value calculated for the case of dry grinding. It is considered to be due to a measurement problem with the power. The effect of the depth of cut on the convection coefficient is shown in Fig. 9, and a similar trend to the results obtained for CI is observed.

## 7 Conclusions

A semiempirical model for the estimation of the convection heat transfer coefficient of fluid through the grinding contact zone has been developed based on the theory of fluid dynamics and heat transfer. The work has shown that the values of the convection coefficient can be very high, much higher than the values previously reported, and change with the grinding parameters. This primary work makes it possible to determine a suitable value of useful flow rate through the grinding contact arc under optimization of the wheel speed, work speed, and jet nozzle velocity.

Although the values of convection heat transfer coefficient presented in this paper can be used as an input in the predictive thermal models and FEA model and the comparisons among the experimental result and the theoretical results predicted by the heat model and FEA model show that $h_f$ is accurate and reasonable, there are still some modifications to be made. The next work we need to do is to modify this model by considering how the side flow of the coolant in the contact area affects the useful flow and how to modify this model by considering surface profile effects of the wheel.

**Acknowledgements** The authors would like to thank Prof. W. B. Rowe, previously of AMTReL, Liverpool John Moores University, for his contributions to this work. The work was supported by EPSRC (grant no. GR/S82350/01) and the National Science Foundation of China (grant no. 50475114).

## References

1. Tawakoli T (1993) High efficiency deep grinding. VDI-Verlag and Mechanical Engineering Publications, UK
2. Andrews C, Howes T, Pearce T (1985) Creep-feed grinding. Holt, Rinehart and Winston, New York
3. Malkin S (1974) Thermal aspects of grinding. Part 1: energy partition. J Eng Ind 96:1177–1183
4. Malkin S (1974) Thermal aspects of grinding. Part 2: surface temperatures and workpiece burn. J Eng Ind 96:1184–1191
5. Guo C, Wu Y, Varghese V, Malkin S (1999) Temperatures and energy partition for grinding with vitrified CBN wheels. Ann CIRP 48(1):247–250
6. Jen TC, Lavine AS (1995) A variable heat flux model of heat transfer in grinding model development. J Heat Transfer 177:473–478 doi:10.1115/1.2822546
7. Demetrious MD, Lavine AS (2000) Thermal aspects of grinding: the case of up-grinding. J Manuf Sci Eng 122:605–611
8. Rowe WB, Pettit JA, Boyle A, Moruzzi JL (1988) Avoidance of thermal damage in grinding and prediction of the damage threshold. Ann CIRP 37(1):327–330
9. Rowe WB, Morgan MN, Allanson DR (1991) An advance in the modelling of thermal effects in the grinding process. Ann CIRP 40 (1):339–342
10. Rowe WB, Morgan MN, Black SCE, Mills B (1996) A simplified approach to thermal damage in grinding. Ann CIRP 45(1):299–302
11. Rowe WB, Black S, Mills B, Morgan MN, Qi HS (1997) Grinding temperatures and energy partitioning. Proceedings: Mathematical, Physical and Engineering Sciences 453:1083–1104
12. Jaeger JC (1942) Moving sources of heat and the temperature at sliding contacts. Proceedings of the Royal Society of New South Wales 76:203–224
13. Outwater JO, Shaw MC (1952) Surface temperatures in grinding. Trans ASME 74:73–78
14. Maris M, Snoeys R (1973) Heat affected zone in grinding operations. Proceedings of the Fourteenth International Machine Tool Design and Research Conference, Manchester
15. Des Ruisseaux NR, Zerkle RD (1970) Temperatures in semi-infinite and cylindrical bodies subject to moving heat sources and surface cooling. J Heat Transfer 92:456–464
16. Verkerk J (1975) The real contact length in cylindrical grinding. Ann CIRP 24(1):259–263
17. Rowe WB, Qi HS, Morgan MN, Zhang HW (1993) The effect of deformation in the contact area in grinding. Ann CIRP 42(1):409–412
18. Werner PG, Younis MA, Schlingensiepen R (1980) Creep-feed—an effective method to reduce workpiece surface temperatures in high efficiency grinding processes. Proceedings of the 8th North American Metal Working Research Conference, SME, pp 312–319
19. Guo C, Malkin S (1992) Analysis of fluid flow through the grinding zone. J Eng Ind 114:427–434
20. Carslaw H, Jaeger JC (1959) Conduction of heat in solids. Oxford University Press, Oxford, UK
21. Rowe WB (2001) Temperature case studies in grinding including an inclined heat source model. Proceedings of the I MECH E Part B Journal of Engineering Manufacture 215(Part B):473–482

22. Douglas JF (1986) Solving problem in fluid mechanics. Longman Scientific and Technical, Singapore
23. Rowe WB, Jin T (2001) Temperature in high efficiency deep grinding (HEDG). Ann CIRP 50(1):205–208
24. Rowe WB (2001) Thermal analysis of high efficiency deep grinding. Int J Mach Tools Manuf 41:1–19 doi:10.1016/S0890-6955(00)00074-2
25. Malkin S (1974) Thermal aspects of grinding. J Eng Ind 96:1184–1191
26. Qi HS (1995) A contact length model for grinding wheel–workpiece contact. Ph.D. Thesis, Liverpool John Moors University, UK
27. Morgan MN, Rowe WB, Black SCE, Allanson DR (1998) Effective thermal properties of grinding wheels and grains. Proceedings of the I MECH E Part B Journal of Engineering Manufacture 212(Part B):661–669
28. Wen LK, Jen FL (2006) General temperature rise solution for a moving plane heat source problem in surface grinding. Int J Adv Manuf Technol 31(3–4):268–277 doi:10.1007/s00170-005-0200-0
29. Pavel R, Srivastava A (2007) A experimental investigation of temperatures during conventional and CBN grinding. Int J Adv Manuf Technol 33(3–4):412–418 doi:10.1007/s00170-006-0771-4